

EXTENSION OF A SIMPLE MATHEMATICAL MODEL FOR ORBITAL DEBRIS PROLIFERATION AND MITIGATION

Jarret M. Lafleur^{*}

A significant threat to the future of space utilization is the proliferation of debris in low Earth orbit. To facilitate quantification of trends and the assessment of potential mitigation measures, this paper extends a previously proposed analytic debris proliferation model consisting of two coupled differential equations. Analyzed are the transient and equilibrium behavior of the parametric model, leading to assessment of the likely effectiveness of potential debris mitigation measures. Results suggest the current equilibrium capacity for intact satellites in low Earth orbit allows for only 25% of the satellites in orbit today and presents an average 2.8% per year risk of catastrophic collision for individual satellites. Results also suggest that direct removal of debris fragments has the potential to add decades or centuries of useful life to low Earth orbit. In addition to providing numerical results, this paper contributes a simple debris model particularly useful when more sophisticated models are unavailable or prohibitively time-consuming to utilize.

INTRODUCTION

On March 17, 1958, a Vanguard rocket carried aloft a small, 6-inch-diameter instrumented sphere known as Vanguard 1, becoming America's second successful attempt at launching a satellite into orbit. Today, Vanguard 1 still orbits Earth, approaching as close as 650 km at perigee and reaching as far as 4,000 km at apogee.¹ Over the five decades that Vanguard 1 has been in orbit, it has been joined by thousands more spacecraft and, more ominously, hundreds of thousands of pieces of debris.^{2,3,4} In densely-populated low Earth orbit (from 200 km to 2000 km altitude), these objects travel at Earth-relative speeds approaching 8 km/s, meaning collisions can occur at relative speeds up to 16 km/s. For comparison, the kinetic energy liberated during a 10 km/s collision with a particle of just a few grams in mass is equivalent to that of a hand-held grenade and can destroy a spacecraft.⁵ Moreover, each collision can produce thousands more pieces of debris, exacerbating the problem.

With little damping from the Earth's atmosphere, the on-orbit collection of satellites and debris has increased dramatically over the past 50 years. It is estimated that 15,000 objects in low Earth orbit (LEO) are larger than 10 cm in diameter and another 100,000 are between 1 cm and 10 cm in diameter, generally considered the threshold for catastrophic damage.^{2,4} These numbers continue to grow. In January 2007, China deliberately destroyed its Fengyun 1C weather satellite in an anti-satellite missile test, instantly increasing the amount of on-orbit debris by 25%.⁴ In February 2009, headlines were made when Russian and American satellites (Cosmos 2251 and Iridium 33, respectively) collided over Siberia, marking the first collision of two intact spacecraft.

It is easily recognized that, without effective mechanisms to remove debris from LEO, the debris population will grow virtually without bound as collisions with debris produce more debris. Debris removal techniques will become necessary. This work seeks to model the orbital debris environment with a set of coupled differential equations, search for stable solutions, and in a top-down manner assess requirements for future debris removal techniques to be effective.

Highlights of Previous Mathematical Modeling Efforts

Multiple approaches exist to modeling the on-orbit debris population. The most accurate approaches involve Monte Carlo analysis using the numerical integration and orbit propagation of all objects for which tracking data currently

^{*} Ph.D. Candidate, School of Aerospace Engineering, Georgia Institute of Technology, Atlanta, Georgia 30332.

exists. This characterizes efforts undertaken, for example, by the SOCRATES system⁶, which produce short-term projections of collisions between individual objects (e.g., to allow satellite operators to perform debris avoidance maneuvers). However, this computationally-intensive approach is difficult to extend for long-term prediction and is difficult to execute without access to databases of currently tracked Earth-orbiting objects and their orbital elements.

In contrast, some analysts have approached the problem from a more simplistic standpoint. A seminal paper on the topic, written in 1978 by Kessler and Cour-Palais, leveraged modeling techniques used to describe formation of the asteroid belt,^{*} developed a single integro-differential equation describing global collision rate as a function of average relative velocity, cross-sectional area, and spatial density of objects.⁷ Fourteen years later, Talent modeled the population of orbiting objects with a single differential equation.⁸ A 1991 paper by Farinella and Cordelli introduced a system of two coupled differential equations to describe the scenario; one equation described the rate of change of the population of intact satellites (N), and the other described the rate of change of the population of debris fragments (n).⁵ This model is given in Eqs. (1)-(2), where A , x , α , and β are constants.

Reference 5 numerically integrated these equations using several assumptions for the coefficients. Results indicated that within 200 years, the number of intact satellites in LEO would decrease dramatically due to collisions with debris (see Figure 1), resulting in an eventual condition in which any satellites launched are quickly destroyed by collisions.

The work of Reference 5 was later extended into various forms (one of which used 150 differential equations, distinguishing satellites by mass and altitude).^{9,10} However, the general results of the original model are accepted as showing good agreement with later studies,^{9,11} and the simpler model remains useful for identifying trends, developing approximations, and establishing instructive models.¹¹ The original model is also useful in distinguishing between intact satellites and debris fragments (rather than aggregating both into one variable). This current work seeks to improve upon the original model through changes to its two differential equations, by considering issues of stability, and by considering effects of debris mitigation techniques not originally analyzed.

Analysis Outline

This analysis is divided into three steps. The first modifies the model of Reference 5 to include additional effects. The second analyzes the equilibrium and stability of the modified model, and the third step uses this model to examine effects debris mitigation strategies may have on improving the stability and equilibrium capacity of LEO.

Step 1: Model Modification. To improve upon the original model of Eqs. (1)-(2), two main modifications are proposed: (1) Separate the A coefficient, which represents the net satellites added to orbit each year, into launch and re-entry terms, each which has a cyclic variation with time (e.g., with the 11-year solar cycle for re-entry and space industry cycles for launch¹²) and (2) add N^2 and n^2 terms representing collisions between intact satellites (as in the Iridium/Cosmos collision) and between fragments, respectively. Coefficients are estimated for these new terms and updated and updating the values of coefficients for the model's original terms. The resulting plot of N and n versus time are compared to the original model's results.

Step 2: Stability Assessment. Using the updated model, equilibrium points are identified and stability is assessed through linearization. A simplified model is developed using nondimensionalization to completely characterize solu-

$$\frac{dN}{dt} = A - xnN \quad (1)$$

$$\frac{dn}{dt} = \beta A + \alpha xnN \quad (2)$$

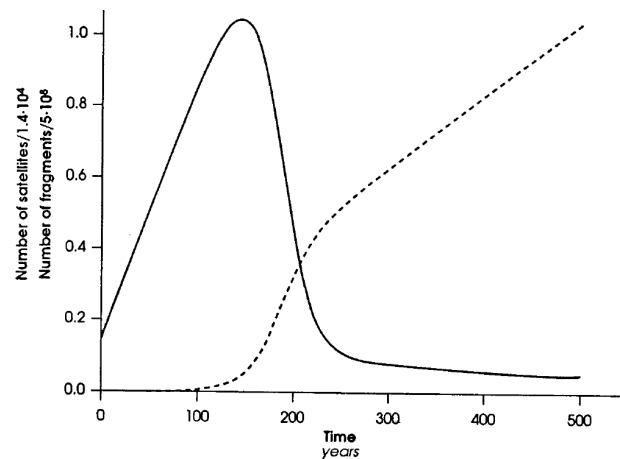


Figure 1. Predicted numbers of intact satellites (solid line) and debris fragments (dashed line) over time, from Reference 5. Note differing y-axis scales for solid and dashed lines.

* The theorized exponential growth of orbital debris and consequent destruction of operational satellites has been termed Kessler Syndrome, after the first author of this original work.⁷

tions by two parameters. Simple analytical expressions are developed for equilibrium points and conditions for oscillatory and nonoscillatory stability. Vector fields akin to phase portraits are plotted, and issues of resonance and time-to-peak are addressed. This step is significant because, with the addition of drag to the model, stable points now exist.

Step 3: Debris Mitigation Implications. The final step in the analysis examines the implications of this model's results on orbital debris mitigation strategy. Common proposals for mitigation strategies involve (1) launching "space tugs" to deorbit intact but inoperative spacecraft or (2) launching giant "nets" of aerogel or similar material to catch or slow debris fragments. The first strategy indirectly slows the formation of fragments by removing one of their sources, while the second strategy has a direct effect on removing fragments from orbit. These methods, as well as others suggested by the data, are examined with an emphasis on estimating effects of practical mitigation measures.

MODEL MODIFICATION

Eqs. (3)-(4) present the proposed modification to the original model of Reference 5. Time is measured in years. This modification, which forms the basis for the rest of this paper, is motivated by the desire to incorporate and observe the importance of effects not originally accounted for in Reference 5. Note several similarities with the original model:

- In Eq. (3), note the existence of a positive term $a + b \sin(ct + d)$, which is the sinusoidally-varying equivalent to the A term in Eq. (1). This term represents the global satellite launch rate to low Earth orbit.
- In Eq. (3), note the preservation of the xnN term from Eq. (1), representing the reduction in the number of intact satellites due to collisions between intact satellites and debris fragments.
- In Eq. (4), the use of the coefficient β multiplied by the satellite launch rate is retained, representing the increase in debris due to upper stage separation processes or explosions.
- In Eq. (4), the use of the coefficient α multiplied by xnN is preserved, representing the increase in debris due to the destruction and fragmentation of intact satellites.

However, inspection of Eqs. (3)-(4) also reveals a number of new terms:

- In both Eqs. (3)-(4), note negative terms proportional to N and n , respectively. These account for annual re-entry of objects from orbit. The periodic variation in the characteristic decay time in these terms is due to the 11-year solar cycle, which produces large density variations in Earth's thermosphere and exosphere.
- Eq. (3) contains an additional term, $2yN^2$, representing the number of intact satellites lost per unit time due to the collision of two intact satellites (as in the February 2009 Cosmos-Iridium collision). Eq. (4) contains the corresponding term γyN^2 , representing the fact that such collisions produce debris fragments.
- Eq. (4) contains an additional term, $2zn^2$, for the rate of destruction of debris fragments due to the collision of two fragments. Here it is assumed such a collision produces debris smaller than the 1 cm threshold.

$$\frac{dN}{dt} = (a + b \sin(ct + d)) - \frac{N}{f + g \sin(ht + k)} - xnN - 2yN^2 \quad (3)$$

$$\frac{dn}{dt} = \beta(a + b \sin(ct + d)) - \frac{n}{p + q \sin(ht + k)} + \alpha xnN + \gamma yN^2 - 2zn^2 \quad (4)$$

It is worth noting here that, unlike the original model of Reference 5, Eqs. (3)-(4) are not autonomous. There exist explicit time dependencies in the launch and re-entry terms. However, it might be hypothesized that, if the sinusoids do not produce resonance, dealing only with average values for these terms may be nearly as accurate and more insightful analytically.* This will be tested in Step 2. The remainder of the present section focuses on the estimation of the coefficients in Eqs. (3)-(4) as well as empirical observations and comparisons involving results of the new model.

Model Coefficient Estimation

Global Launch Rate. One update incorporated into this new model is a revised global launch rate for LEO satellites. Using data from Hiriart and Saleh¹², this launch rate is illustrated in Figure 2. Notice the large increase in launch rate in the early 1960s and a high launch rate through the 1980s. At the end of the Cold War, launch rate decreased substantially, with the main exception in the late 1990s with the fielding of the Iridium constellation.

* This will amount to a rudimentary homogenization; future work may consider further development of this aspect.

Importantly, the original model of Reference 5 assumed the LEO launch rate would remain 100 satellites per year. This appeared a fair approximation in 1991, for which the data of Reference 12 shows 83 satellites launched.* However, today this rate is considerably smaller, averaging 30.5 per year since 2001.

Another inaccuracy with the launch rate of Reference 5 is that it is assumed constant. While it is difficult to predict satellite launch rates, improvements may be made by taking advantage of the recent work of Reference 12, which highlights the empirical existence of cycles in global launch rates. In particular, Reference 12 found identified 3-year cycles among defense, science, and communications satellite launches over the past decade.

The black line in Figure 3 represents the global LEO launch rate since 2001. While Reference 12 utilized Fourier transforms, the simplified approach here uses a single-frequency sinusoid to capture a 3.3-year cycle. The resulting sinusoid is the gray line in Figure 3. With $R^2 = 0.65$, this model explains recent launch rate variations more accurately than a simple average and is adopted for this work. The equation for the launch rate sinusoid is given in Eq. (5), where LR is equivalent to A in the model of Reference 5 and $t = 0$ is referenced to the year 2009.

$$LR = a + b \sin(ct + d) = 31.41 + 7.794 \sin(1.935t + 0.1680) \quad (5)$$

Atmospheric Re-entry Rate. One omission in the original model of Reference 5 was the decrease in satellite and fragment populations due to atmospheric drag and re-entry. While atmospheric density in LEO is orders of magnitude smaller than at Earth's surface, when integrated over a period of years this drag results in a satellite or fragment trajectory that spirals inward until re-entry and disintegration. Furthermore, the atmospheric density in LEO is substantially affected by the 11-year solar cycle, observed consistently since the 17th century.¹³ Large density increases during solar maximum periods have, for example, subtracted years from the lifetimes of the Salyut 7 and Skylab space stations.¹⁴

Figure 4 shows the result of using an atmospheric model¹⁵ to compute on-orbit lifetime for intact satellites and debris fragments for solar maximum and minimum conditions. The solid lines in Figure 4 indicate orbital lifetime estimates for a static solar maximum model, and the dashed lines indicate orbital lifetime for solar minimum conditions. The difference between the models is substantial: An intact satellite at 800 km altitude has an orbital lifetime of about 100 years for the solar maximum atmosphere and over 1000 years for solar minimum.

As shown in Figure 4, the orbital lifetime computed for intact satellites assumes a ballistic coefficient of 110 kg/m^2 , an average value for satellites.^{15,16} The orbital lifetime for debris fragments assumes a ballistic coefficient of 1.8 kg/m^2 , an approximate average value for fragments derived from Reference 17. The ballistic coefficient B , defined as the ratio of object mass to the product of reference area and drag coefficient (i.e., $B = m/(C_D A)$), differs significantly for intact satellites and fragments because fragments typically have larger surface-area-to-volume ratios. As Figure 4 shows, the smaller ballistic coefficient of fragments produces a two-order-of-magnitude reduction in orbital lifetime (helpful from the perspective of orbital debris mitigation). For example, at 800 km altitude, the orbital lifetime of an intact satellite is about 100 years for solar-maximum conditions, while the orbital lifetime of a fragment is just over one year.

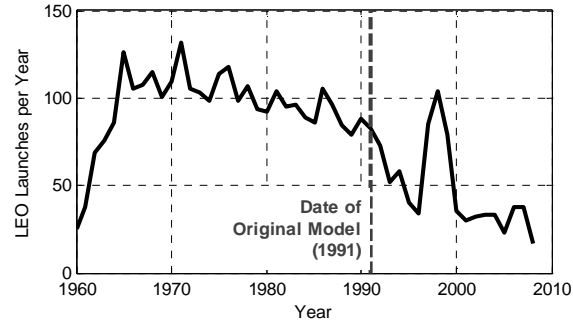


Figure 2. Global launches to LEO per year since 1960. Note the substantial decrease in launch rate after 1991.

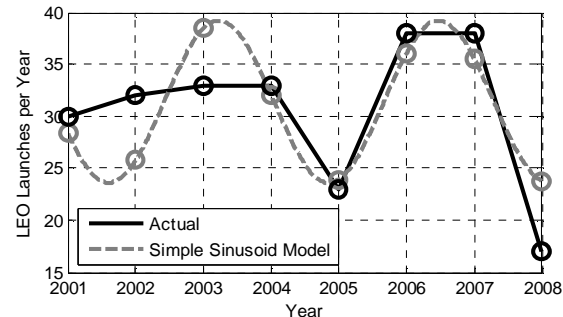


Figure 3. Global launches to LEO since 2001. Overlaid is a sinusoid model, determined through least-squares fit.

* The data of Reference 12 does not include manned launches, for example, which are short-lived and can reasonably be neglected as debris contributors. Reference 12 reports its database is 83.5% complete; if the 83 launches in 1991 is corrected by this factor, the data suggest 99 launches in 1991, almost exactly the 100-satellite rate of Reference 5.

With atmospheric drag effect now quantified via orbit lifetime, this work utilizes the approach of Reference 9, which models the rate of change of orbiting satellites as a function of the number of current satellites divided by a time constant τ . This time constant is the orbital lifetime of the satellites (implying that if 1000 satellites are on-orbit and each has a 1000-year orbital lifetime, the expected decay and re-entry rate is one satellite per year).*

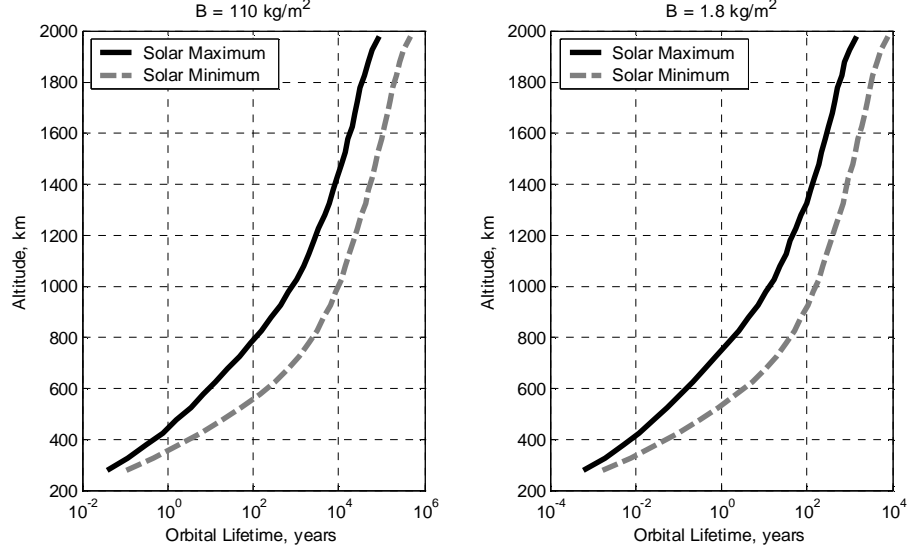


Figure 4. Expected orbital lifetime for intact satellites ($B = 110 \text{ kg/m}^2$, left) and debris fragments ($B = 1.8 \text{ kg/m}^2$, right). These lifetimes are computed assuming a static atmosphere at the indicated solar maximum or minimum level.

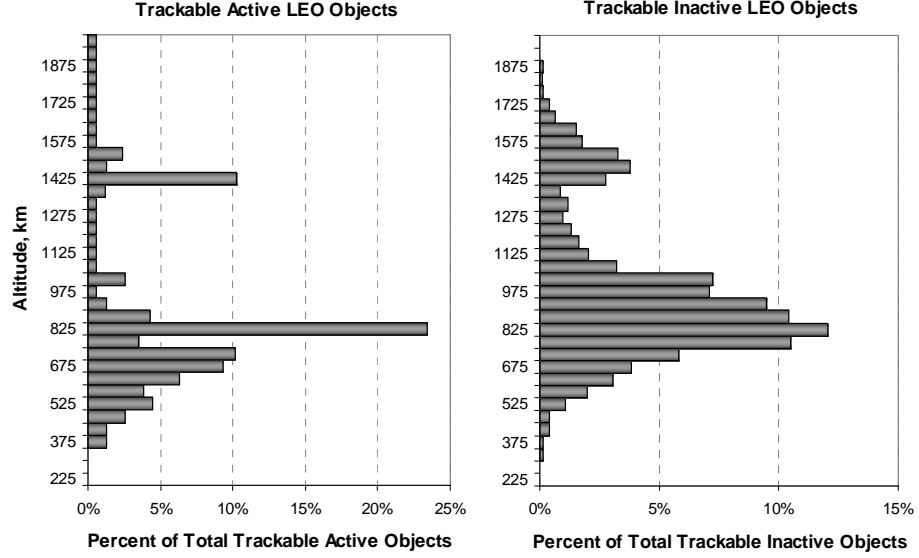


Figure 5. Current Distribution of Trackable Active (left) and Inactive (right) Objects in LEO.

* This assumption has some limitations, for example, if there are surges in launch rate. In the previous example, had all 1000 satellites been launched in the same year, all would re-enter 1000 years later rather than one per year. However, this assumption is reasonable if the satellite population exhibits a diversity of launch dates. Another limitation of this assumption is that it does not account for reboot orbit maintenance maneuvers. This is accurate for debris fragments and inactive spacecraft but is not always true for active spacecraft (in which case this assumption would produce optimistic estimates in terms of debris mitigation, since spacecraft in the model deorbit more quickly than those in reality).

For this analysis, two such τ parameters are required, representing the average orbital lifetime for intact satellites and for debris fragments. To determine these parameters, the orbital lifetimes from Figure 4 are weighted by the distribution of objects at different orbital altitudes and averaged. The current distribution of active trackable LEO objects⁴ is applied to the intact satellites (with $B = 110 \text{ kg/m}^2$), and the current distribution of inactive trackable LEO objects⁴ is applied to the debris fragments (with $B = 1.8 \text{ kg/m}^2$). These distributions are shown in Figure 5. This average is computed for both solar maximum and solar minimum conditions. At solar maximum, the average orbital lifetime of intact satellites is found to be $\tau_{\text{intact}} = 3,990$ years and the average lifetime of debris fragments is found to be $\tau_{\text{debris}} = 46.9$ years. At solar minimum, the average orbital lifetime of intact satellites is found to be $\tau_{\text{intact}} = 24,840$ years and the average lifetime of debris fragments is found to be $\tau_{\text{debris}} = 322.8$ years.

To account for the time-varying nature of τ due to the 11-year solar cycle, a sinusoid is used. The period of the sinusoid is set to 11 years, and the phase shift is set to match the predicted 2013 solar maximum (with $t = 0$ indicating the year 2009). The amplitude and average values are selected to match the values of τ_{debris} and τ_{intact} at solar maximum and minimum. The resulting models for τ_{debris} and τ_{intact} are shown in Eqs. (6)-(7):

$$\tau_{\text{intact}} = f + g \sin(ht + k) = 14,420 - 10,430 \sin(0.5712t - 0.9996) \quad (6)$$

$$\tau_{\text{debris}} = p + q \sin(ht + k) = 184.9 - 137.9 \sin(0.5712t - 0.9996) \quad (7)$$

Collision Terms. The final revision to the model of Reference 5 is addition of terms accounting for collisions among intact spacecraft and among fragments. Following the modeling strategy of Reference 5, this work approximates collision probabilities in the manner that the gas dynamics community approximates collision rates among molecules. In particular, collision frequency ξ for a single molecule A with other molecules is the product of effective cross-sectional area σ , molecular velocity v , and number of molecules n per unit volume V , shown in Eq. (8) (cf. Reference 18).

$$\xi = \frac{\sigma n \bar{v}}{V} \quad (8)$$

If collisions of interest are between molecules of different types (e.g., collisions of molecule type A with type B), the total collisions per unit time is ξ multiplied by the number of A molecules in the system, given by Ξ_{AB} in Eq. (9). If collisions of interest are between like molecules, the total collision rate Ξ_{AA} is as shown in Eq. (10) (cf. Reference 18). Note that cross-sectional area is computed using the average diameter of the two molecules of interest, so $\sigma_{AB} \neq \sigma_{AA}$.

$$\Xi_{AB} = \frac{\sigma_{AB} n_A n_B \bar{v}}{V} \quad (9)$$

$$\Xi_{AA} = \frac{\sigma_{AA} n_A^2 \bar{v}}{2V} \quad (10)$$

For objects in LEO, this formulation is conducive to collision rate approximations with minimal information. Cross-sectional area is estimated by approximating satellites as spheres with a 2.2 m diameter based on average diameters from 26 satellites.^{1,15,19,20,21,22,23,24} Fragments are optimistically modeled as spheres of 1 cm diameter, the smallest fragments likely to cause catastrophic damage. As a result, intact-intact object collisions use $\sigma_{NN} = 14.9 \text{ m}^2$, intact-debris collisions use $\sigma_{Nn} = 3.77 \text{ m}^2$, and debris-debris collisions use $\sigma_{nn} = 3.14 \text{ cm}^2$.

Average velocity is estimated based on weighted averages of satellite circular orbit speed, which varies from 6.89 km/s at 2000 km altitude to 7.77 km/s at 200 km altitude. For intact satellites, these speeds are weighted by the distribution of active spacecraft from Figure 5, yielding an average speed of 7.39 km/s. For debris fragments, these speeds are weighted by the distribution of inactive tracked objects from Figure 5, yielding an average speed of 7.36 km/s. For the case of intact-debris collisions, the velocity used is the average of these two, or 7.37 km/s.

The relevant volume in this application is the volume of the 200-2000 km orbital shell, calculated by subtracting the volumes of the inner and outer spheres. This yields $V = 1.27 \times 10^{12} \text{ km}^3$.

The annual per-fragment and per-satellite collision probabilities x , y , and z that result when these values are substituted in Eq. (10) are given in Eqs. (11), (12), and (13). Note that, since Ξ_{NN} and Ξ_{nn} represent the frequency of collisions among like object types (intact satellites and fragments), each collision results in the loss of *two* objects. This is accounted for by a multiplicative factor of two in the appropriate places in Eqs. (3)-(4). Also, note that the independently-calculated $6.895 \times 10^{-10} \text{ yr}^{-1}$ -fragment⁻¹ value for x shows reasonable agreement with the $3 \times 10^{-10} \text{ yr}^{-1}$ -fragment⁻¹ value assumed by Reference 5, which had been founded on a similar gas-dynamics-based estimate.

$$\Xi_{Nn} = xnN = 6.895 \times 10^{-10} nN \quad (11)$$

$$\Xi_{NN} = yN^2 = 1.369 \times 10^{-9} N^2 \quad (12)$$

$$\Xi_{nn} = zn^2 = 2.869 \times 10^{-14} n^2 \quad (13)$$

As an additional check, it is straightforward to convert these Ξ -values to annual collision probabilities. Based on this data, the current annual probability of collision with a debris fragment for an intact satellite is $P_n = xn_0$, where n_0 is the current number of fragments (of >1 cm diameter) in orbit. In this work, n_0 is estimated at 110,400,^{2,4,25} yielding $P_n = 7.61 \times 10^{-5}$ per year, which is in reasonable (and somewhat optimistic) agreement with altitude-dependent 10^{-5} to 10^{-2} annual LEO collision probability estimates from Reference 15. Additionally, the annual probability of collision with an intact satellite can be computed as $P_N = 2yN_0$, where N_0 is the current number of intact satellites in orbit. Here, N_0 is estimated at 4,650,²⁵ yielding $P_N = 1.27 \times 10^{-5}$ per year, which is also in reasonable agreement with corresponding altitude-dependent 10^{-6} to 10^{-3} annual LEO collision probability estimates from Reference 15.

The final parameters to estimate are the empirical fragmentation parameters β , α , and γ . The parameter β represents the average number of fragments released per launch. These fragments primarily consist of unintended post-launch propellant tank explosions, but this also includes discarded components such as shrouds, lens covers, and separation devices. This study retains Reference 5's original estimate of $\beta = 70$.

The parameter α represents the average number of fragments produced from the collision of debris with an intact satellite. This number is empirical, and this study retains Reference 5's original estimate of $\alpha = 10,000$. Related to α is the new parameter γ , representing the average number of fragments produced from the collision of two intact satellites. Empirical evidence for this is scarce; based on the 2009 Iridium-Cosmos collision, this is estimated at $\gamma = 56,000$.²⁶

Summary of Coefficients. Table 1 summarizes all terms developed here, applicable to Eqs. (3)-(4).

Table 1. Summary of Coefficient and Initial Condition Point Estimates.

Coefficient	Point Estimate	Units	Coefficient	Point Estimate	Units
a	31.41	satellites / year	x	6.895×10^{-10}	year ⁻¹ · fragment ⁻¹
b	7.794	satellites / year	y	1.369×10^{-9}	year ⁻¹ · satellite ⁻¹
c	1.935	radians / year	z	2.869×10^{-14}	year ⁻¹ · fragment ⁻¹
d	0.1680	radians	α	10,000	fragments / satellite
f	14,420	years	β	70	fragments / satellite
g	-10,430	years	γ	56,000	fragments / satellite
h	0.5712	radians / year			
k	-0.9996	radians	N_0	4,650	satellites
p	184.9	years	n_0	110,400	fragments
q	-137.9	years			

Results of the Nominal Model

Before proceeding with stability analysis of the new model, this study first examines the model's behavior in the time domain. The black lines in Figure 6 show the behavior of the new model over a 500-year period, the time span used by Reference 5.* Gray lines show data reproduced from Reference 5, starting from 1991 (the date of Reference 5).

Looking first at the upper plot in Figure 6, it is worth noting that the revised model predicts substantially fewer intact satellites in LEO at the peak. The original model predicts a peak population of 14,500 in the year 2137, while the revised model predicts a peak population of 6,900 in the year 2108. The two models agree in the year 2021, but as will be shown in more depth later, the lower global launch rate in the revised model (the only positive term in the dN/dt equation) causes a slower rise and a smaller peak. It is also important to recognize that while the original model predicts a continuously declining population, the revised model indicates a recovery period beginning in the late 23rd century which appears to equilibrate at a level of 1100 intact satellites.

The lower plot in Figure 6 shows the proliferation in the number of >1 cm debris fragments with time. Here, differences between the original and revised models are even more striking: The two models agree closely until the mid-22nd century. However, because the original model of Reference 5 included no atmospheric drag, the gray line continues

* These plots result from numerically integrating Eqs. (3)-(4) using MATLAB's *ode45* with 10^{-6} relative tolerance.

upward without limit. In contrast, the black line appears to overshoot equilibrium and then decay. Oscillations in this line are due to the 11-year solar cycle. At the peak in 2210, there are 64.7 million fragments in LEO, over 500 times as many as exist today. At this level, the average probability of collision with a debris fragment in LEO becomes 4.5% per year, compared to 0.0076% per year today. With a 4.5% annual risk, a new satellite can be expected to be destroyed, on average, 22 years after launch.

It might be hypothesized that some terms in Eqs. (3)-(4) have negligible contributions to the on-orbit satellite and debris population within the timeframe considered in this study. In an effort to empirically identify negligible contributors to the system's behavior, Figure 7 displays the relative contributions to the dN/dt and dn/dt terms as a function of time. The upper plot in Figure 7, for example, shows the relative magnitudes of the four terms in Eq. (3) over time. The fifth curve, colored black, shows the sum of the first four. Notice that the light-gray solid line and darker gray dashed line dominate the plot, while the light-gray dashed line and darker gray solid line are virtually zero for all time. This indicates that collisions between intact satellites and orbit decay of intact satellites are negligible effects, while behavior of the intact satellite population is governed primarily by launch rate and collisions with debris.

The lower plot of Figure 7 shows the relative magnitudes of the five terms in Eq. (4) over time. The sixth curve, colored black, shows the sum of these. Notice that the darker gray dashed line and darker gray solid line dominate the plot, while the light-gray solid line, light-gray dashed line, and black dashed line are virtually zero for all time. This suggests that the number of orbiting debris fragments is governed primarily by orbit decay and collisions between intact spacecraft and debris fragments.

ASSESSMENT OF EQUILIBRIUM AND STABILITY

Several interesting and useful implications of the revised model can be observed through analysis of the system's equilibrium points. The results generated thus far suggest that for the particular selection of the 18 parameters for this model, the number of intact satellites in LEO gradually converges to approximately 1100 and the number of debris fragments converges to 40 million. This suggests the existence of a stable equilibrium point, but it provides no information about how this equilibrium point varies or whether it remains stable for different values of the 18 parameters. The following discussion addresses these questions.

Equilibrium with Sinusoids Removed

To identify equilibrium points, it is necessary to simplify Eqs. (3)-(4) of the revised model into an autonomous set of ordinary differential equations. This requires the removal of the sinusoidal forcing terms in launch rate and re-entry rate. Unfortunately, as visible in Figure 7, these terms are not small in all cases. As noted earlier, the effects of launch

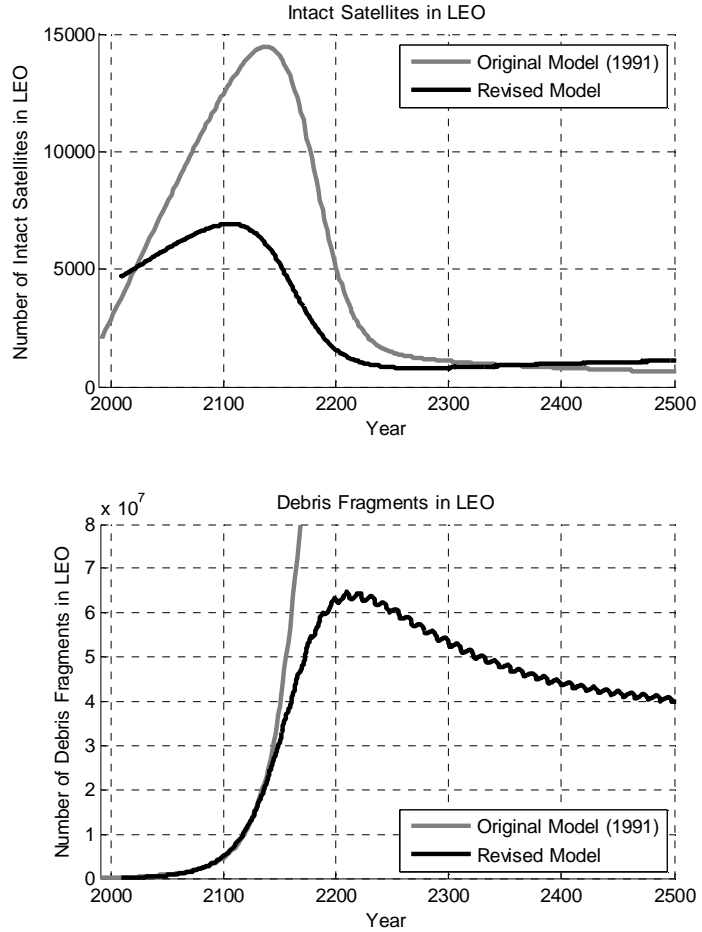


Figure 6. Comparison of the revised model with the original model of Reference 5. The steady-state oscillations visible in the lower plot of the revised model correspond to solar cycle oscillations.

rate on dN/dt and re-entry rate on dn/dt are relatively small, but the effects of launch rate on dN/dt and re-entry rate on dn/dt are substantial. In removing these terms, it is assumed the average launch and re-entry rates are adequate in describing the system's behavior.

Equations (14)-(15), which omit the sinusoidal forcing terms (by setting $b = g = q = 0$), are plotted as the dashed gray lines in Figure 8. Notice that this model and the baseline revised model of Eqs. (3)-(4), shown by the solid black lines, agree closely for the first 100 years of the simulation. The end behavior is also qualitatively the same. In both models, the number of intact satellites in LEO peaks in the early 22nd century, reaches a low in the late 23rd century, and then recovers slightly. Both models also show that the number of debris fragments peaks in the early 23rd century and gradually declines to an equilibrium. Quantitatively, however, the final values of n and N are discrepant by about 50%.

To compensate for this discrepancy, the average time constant for orbital debris re-entry is modified to $p = 130$ years (instead of $p = 184.9$ years). The resulting system response, shown as the solid gray line in Figure 8, shows satisfactory agreement with the baseline model, and this new value for p will be used for the remainder of this paper in instances where sinusoidal terms are removed.

Figure 9 shows the direction field in the n vs. N phase space corresponding to the simplified model of Eqs. (14)-(15), with $p = 130$ years. The black line is the path from the $N_0 = 4,650$ and $n_0 = 110,400$ initial conditions. Note the equilibrium point near $N = 1100$ and $n = 40$ million.

To find the exact coordinates (N^*, n^*) of the equilibrium point, dN/dt and dn/dt in Eqs. (14)-(15) may be set to zero. Setting $dN/dt = 0$ and solving for n^* yields Eq. (16). Setting $dn/dt = 0$ and solving for N^* using the quadratic formula yields Eq. (17). Importantly, the square root term in Eq. (17) must be larger than $\alpha x n^*$ if one of the N^* solutions is to be positive and meaningful. The smaller root of N^* is negative and non-physical.

Solving using the positive root of N^* yields $N^* = 1107.9$ and $n^* = 41.015$ million. Note that this corresponds well to the equilibrium in Figure 9. No other physically meaningful equilibria appear to exist.

As is clear from Eqs. (16)-(17), the analytic expressions for the equilibrium point coordinates are complicated. Stability analysis would introduce further complication. As will be shown in the next section, these expressions can be

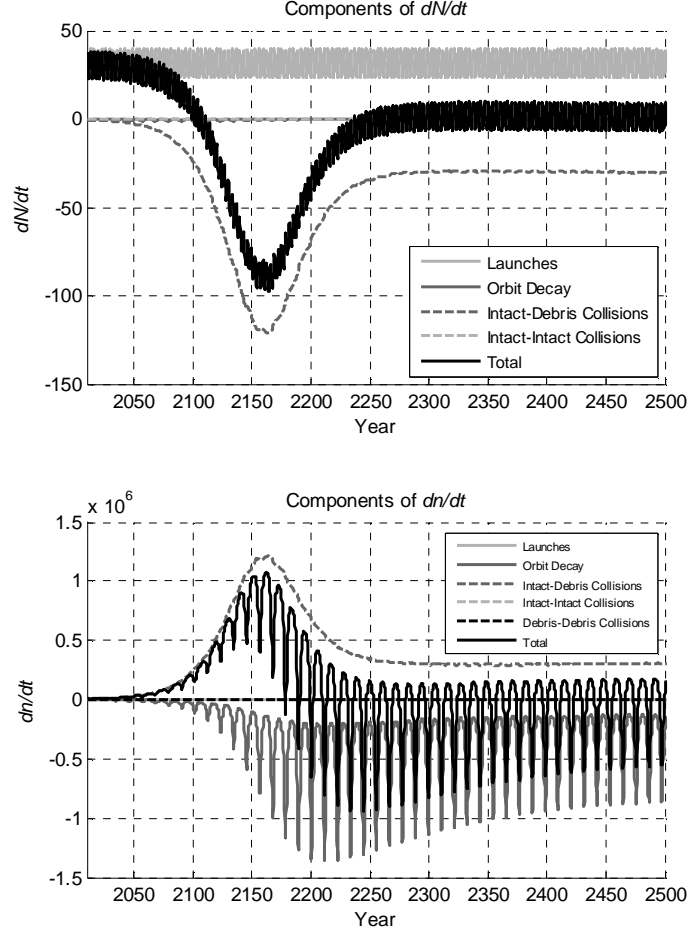


Figure 7. Relative contributions of terms in the revised model. The oscillations in dN/dt are governed by 3.3-year launch cycles, while oscillations in dn/dt are governed by 11-year solar cycles.

$$\frac{dN}{dt} = a - \frac{N}{f} - xnN - 2yN^2 \quad (14)$$

$$\frac{dn}{dt} = \beta a - \frac{n}{p} + \alpha xnN + \gamma yN^2 - 2zn^2 \quad (15)$$

$$n^* = \frac{1}{x} \left(\frac{a}{N^*} - \frac{1}{f} - 2yN^* \right) \quad (16)$$

$$N^* = \frac{1}{2\gamma} \left(-\alpha xn^* \pm \sqrt{\left(\alpha^2 x^2 + 8\gamma z \right) n^{*2} + \frac{4\gamma}{p} n^* - 4\beta a \gamma} \right) \quad (17)$$

simplified by dropping small terms without significant loss of fidelity. Stability behavior is then analyzed for the simplified system.

Equilibrium and Stability for a Simplified System

The goal of this section is to analyze a model that demonstrates similar characteristics to the original model but is simple enough to yield useful analytical expressions for equilibrium and stability behavior. To accomplish this, earlier discussion regarding contributors to dN/dt and dn/dt is leveraged. Recall that in Figure 7, dN/dt was negligibly affected by collisions between and orbit decay of intact satellites. Thus, in the simplified model of Eq. (18), these terms are removed (or equivalently, $y \rightarrow 0$ and $f \rightarrow \infty$). Recall also that dn/dt was negligibly affected by launch rate, collisions between satellites, and collisions between fragments. As a result, the simplified model of Eq. (19) neglects the latter two of these terms (or equivalently sets $y = 0$ and $z = 0$). The βa term is retained for later analysis of policies to improve the orbital debris situation.

The resulting simplified model is shown in Eqs. (18)-(19), and a comparison of the solution of the simplified model to the baseline model without sinusoidal forcing (Eqs. (14)-(15)) is shown in Figure 10. Note the similarity of Eqs. (18)-(19) to the original model of Reference 5 in Eqs. (1)-(2). In effect, by starting with a complicated model and neglecting terms based on their relative contributions, this analysis has independently confirmed the basic model of Reference 5 – but with one key exception. The new model contains a negative term in the dn/dt equation due to the orbital decay of fragments. This term introduces an equilibrium point which, as will be shown, in most cases is asymptotically stable. This significantly changes the character of the end behavior of the solution.

Nondimensionalization. As is clear from Eqs. (18)-(19), the simplified model contains a total of five terms describing dN/dt and dn/dt . There are three variables in the system (N , n , and t), so a nondimensionalization scheme can be selected to produce a system that can be completely described by two parameters. Solving for appropriate normalizing parameters yields the system in Eqs. (20)-(23). Using the parameters in Table 1 (except with $p = 130$ years as discussed earlier), $\chi = 3.660$ and $\rho = 0.007$. Both χ and ρ are unitless. Parameter χ , which characterizes the severity of the debris scenario, consists entirely of quantities (x , a , p , and α) that produce a less desirable debris scenario when increased. The “debris ratio”

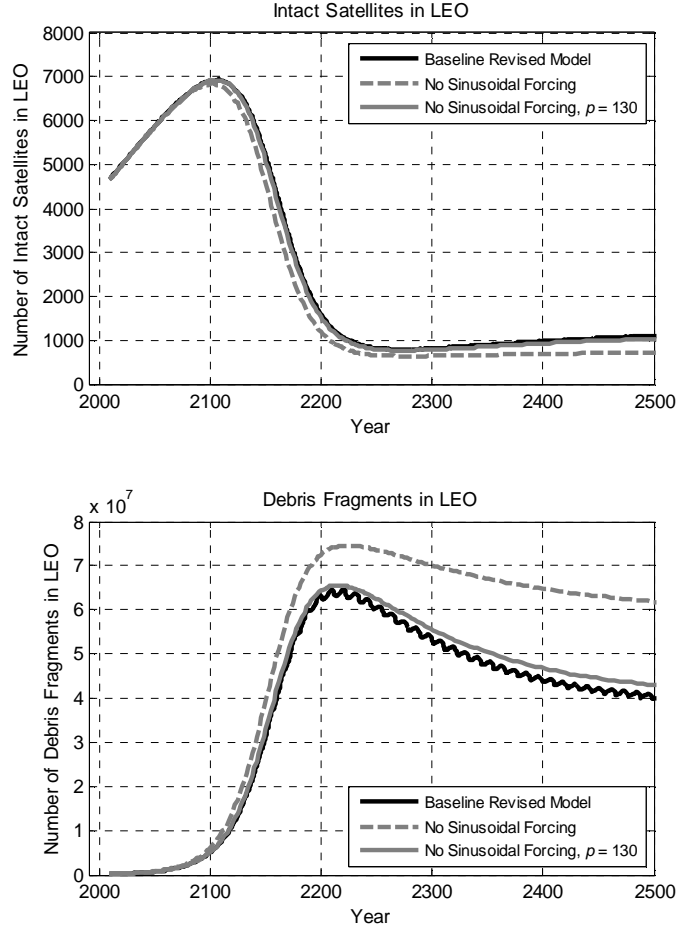


Figure 8. Comparison of model behavior with sinusoidal forcing (solid black line), without sinusoidal forcing (dashed gray line), and without sinusoidal forcing but with a modified p coefficient (solid gray line).

$$\frac{dN}{dt} = a - xnN \quad (18)$$

$$\frac{dn}{dt} = \beta a - \frac{n}{p} + \alpha xnN \quad (19)$$

$$\frac{dM}{ds} = 1 - \chi \rho Mm \quad (20)$$

$$\frac{dm}{ds} = 1 - m + \chi Mm \quad (21)$$

$$\chi = xap^2\alpha \quad \rho = \frac{\beta}{\alpha} \quad (22)$$

$$M = \frac{N}{ap} \quad m = \frac{n}{p\beta a} \quad s = \frac{t}{p} \quad (23)$$

parameter ρ is the ratio of average debris released per launch to average debris released during a collision between a fragment and satellite.

The variables M , m , and s (nondimensional versions of N , n , and t) are all of an order of magnitude between 0.10 and 10 for the solution using the baseline initial conditions. For example, $M_0 = N_0/(ap) = 1.138$, $m_0 = n_0/(p\beta a) = 0.3861$, and $s_{max} = t_{max}/p = 3.85$. Note that the small value of $\chi\rho$ ($= 0.0256$) explains the initial linear growth in the number of intact satellites, visible in Figure 10. As Eq. (20) shows, if $\chi\rho$ is zero, $dM/ds = 1$ and this growth is exactly linear.

Determination of Equilibrium Points. From the simplified equations above, it is straightforward to solve for equilibrium points. Setting dM/ds and dm/ds to zero yields Eqs. (24)-(26). Inserting $\chi = 3.660$ and $\rho = 0.007$ yields $M^* = 0.2713$ and $m^* = 143.9$, the only equilibrium point of the system. Translating into dimensional quantities N^* and n^* yields $N^* = 1107.9$ satellites and $n^* = 41.120$ million fragments. These values are almost identical to those from the more complicated model from Eqs. (14)-(15).

In the case of $\rho \ll 1$, which is reasonable on physical grounds and given the baseline $\rho = 0.007$ value, the formulas for N^* and n^* simplify further to the versions denoted after the “ \sim ” symbol in Eqs. (25)-(26).^{*} In this case, $N^* = 1115.7$ satellites and $n^* = 40.834$ million fragments, which is still very close to the values from the higher-fidelity model.

Interestingly, Eqs. (25)-(26) show the equilibrium value of M is almost entirely governed by χ , and the equilibrium value of m is entirely governed by ρ . This is convenient, although care should be taken in interpreting this result. For example, χ is proportional to launch rate a and M^* is roughly proportional to $1/\chi$, so doubling launch rate roughly halves M^* . However, this does not necessarily halve N^* since N^* has been normalized by the product of launch rate and characteristic fragment orbit decay time. The result is that, while M^* does halve when a is doubled, N^* does not change. Thus, it is worth emphasizing, for example, that greater values of M translate into greater values of N only when all parameters remain constant.

As Eq. (25) shows, the equilibrium value of N is primarily governed by the intact-fragment collision probability x , the characteristic fragment orbit decay time p , and the number of fragments produced per launch α . The number of fragments produced per launch β plays a small role if it is much smaller than α . Equation (26) shows the equilibrium value of n is primarily governed by the characteristic fragment orbit decay time p , global launch rate a , and the number of fragments produced per launch β . As in Eq. (25), the number of fragments produced per launch β plays a small role if it is much smaller than α . Interestingly, note launch rate plays no role in setting the equilibrium value of N . Equally surprising, the collision probability x plays no role in determining the equilibrium value of n .

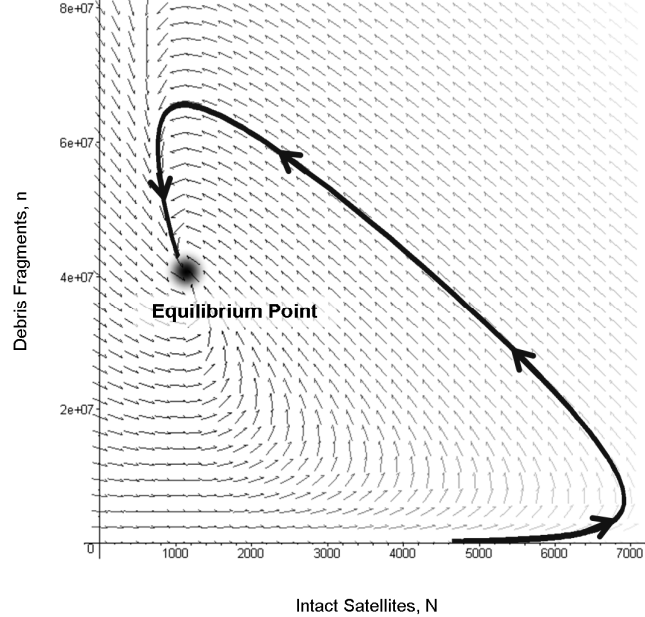


Figure 9. Direction field of the no-sinusoid model. The stable equilibrium point is shown as well as the path traced with the actual initial conditions (the solid black line).

$$M^* = \frac{1}{\chi\rho \left(1 + \frac{1}{\rho}\right)} \sim \frac{1}{\chi} \quad m^* = 1 + \frac{1}{\rho} \sim \frac{1}{\rho} \quad (24)$$

$$N^* = apM^* = \frac{1}{xp\beta \left(1 + \frac{\alpha}{\beta}\right)} \sim \frac{1}{xp\alpha} \quad (25)$$

$$n^* = p\beta am^* = p\beta a \left(1 + \frac{\alpha}{\beta}\right) \sim pa\alpha \quad (26)$$

^{*} Throughout the rest of this work, “ \sim ” indicates a limit as ρ (or β , where appropriate) approaches zero. This is identical to the limit as Q , which will be introduced as $Q = \rho + 1$, approaches unity.

Stability of the Equilibrium Point. With the equilibrium point of the simplified system identified, an important question to address is whether the point is stable and, if so, under what conditions. To address this, the system is linearized about the equilibrium point. The eigenvalues of the linear system are given in Eq. (27), where $Q = \rho(1+1/\rho)$ to simplify notation. For $\rho \ll 1$, $Q \sim 1$ and for $\rho > 0$, $Q > 1$.

Stability for $\chi > 0$ and $Q \sim 1$. The most important observation from Eq. (27) is that, due to the $-4\chi Q$ term, the square root term is always smaller than the $(\chi Q + 1 - 1/Q)$ term to the left of the square root if $\chi > 0$ and $Q > 0$. Because of this and the fact that $(\chi Q + 1 - 1/Q)$ is positive and preceded by a negative sign, both eigenvalues are guaranteed to be negative. No positive values of χ or Q (or ρ) can cause instability. This covers most scenarios since both χ and Q are generally positive quantities.

Equation (28) approximates the eigenvalues of the linear system under the assumption that $Q \sim 1$. This equation reveals more clearly that, although the eigenvalues can never be positive, they can take complex values if $0 < \chi < 4$.

Figure 11 illustrates the behavior of the system in the m vs. M phase space for scenarios in which $\chi = 3.660$ is decreased or increased by a factor of 10 (with ρ fixed at 0.007). The left plot shows oscillatory behavior and the right plot does not, as expected from the $0 < \chi < 4$ condition. The $\chi = 3.660$ behavior is well illustrated by Figure 9, though this case is close to $\chi = 4$ and the oscillatory behavior is only slight. If translated into a change in launch rate (since χ is directly proportional to a), the implication is that an increase in launch rate by just 3 satellites per year would remove the oscillatory behavior; that is, the baseline scenario is only borderline oscillatory.

An additional note regarding stability for this system arises because of the potential oscillatory behavior for $0 < \chi < 4$. It may be recalled that the simplified model does not include the effects of sinusoidal forcing, which raises the question of whether these terms could produce resonance. While linear stability analysis does not apply far from the equilibrium point, it is possible to examine the resonance issue in the area of the equilibrium point.

Based on Eq. (28), the most negative value that $\chi^2 - 4\chi$ can take is -4 . Thus, the largest possible imaginary part of the eigenvalue λ is $\pm i$. As a result, the highest possible frequency of a sinusoid for the local homogeneous solution is 1 radian per nondimensionalized time unit s . This corresponds to a dimensional frequency of 0.00769 radian/year, or equivalently an 817-year period. Thus, given an unfortunate value of χ , resonance is locally possible if a sinusoidal forcing function exists with a period of 817 years or more. It is impossible for periods shorter than this (e.g., the 11-year solar cycle and 3.3-year launch cycle periods).

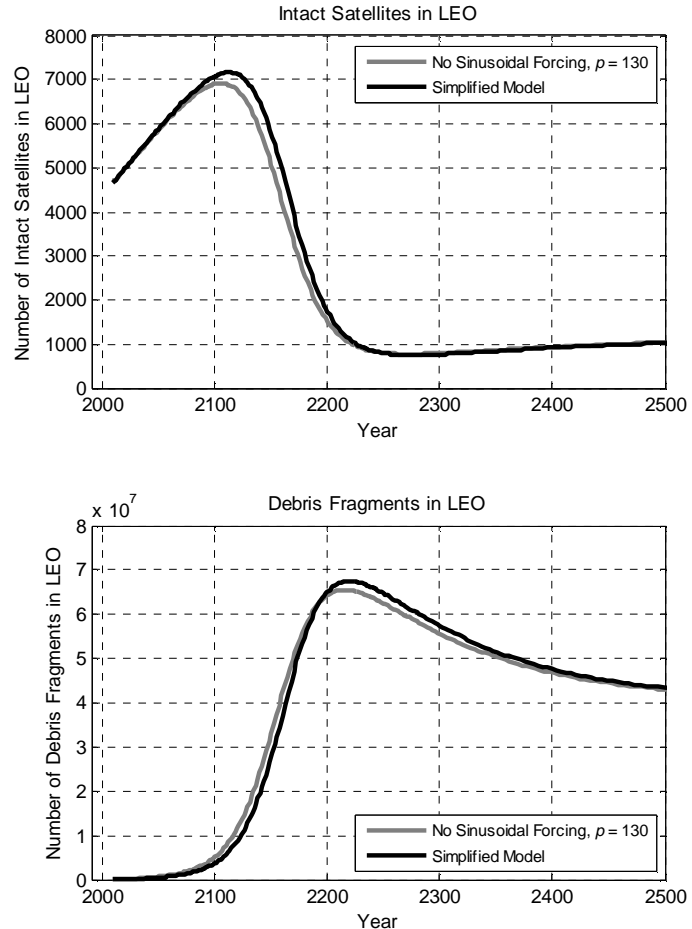


Figure 10. Comparison of model behavior without sinusoidal forcing and with $p = 130$ years (gray line), and without negligible terms (black line).

$$\lambda = \frac{1}{2} \left(-\left(\chi Q + 1 - \frac{1}{Q} \right) \pm \sqrt{\left(\chi Q + 1 - \frac{1}{Q} \right)^2 - 4\chi Q} \right) \quad (27)$$

$$\lambda \sim \frac{1}{2} \left(-\chi \pm \sqrt{\chi^2 - 4\chi} \right) \quad (28)$$

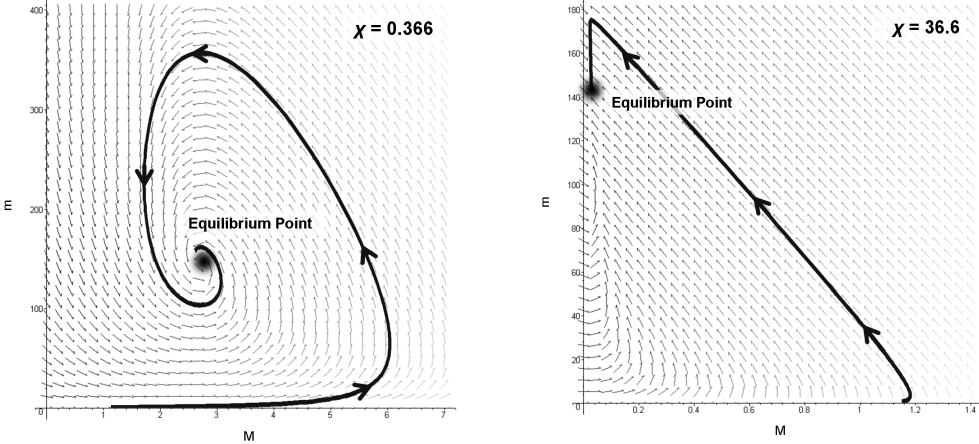


Figure 11. Direction fields of the simplified model with $\chi = 0.366$ (left) and $\chi = 36.6$ (right). Note the oscillatory behavior for the case in which $0 < \chi < 4$. Also note that the axes of the plots have different limits.

General Stability. While the discussion above applies to most practical scenarios, some interest in stability may exist for special cases outside of the $\chi > 0$ and $Q \sim 1$ regime. Based on Eq. (27), Figure 12 shows the equilibrium point's behavior over a wider range of χ and ρ . Black lines indicate the boundaries between stable and unstable regions and gray lines indicate the boundaries between oscillatory and non-oscillatory regions. As expected, the $\chi > 0, \rho > 0$ region is entirely stable, and the baseline equilibrium point is near the oscillation boundary, which crosses the ρ axis at $\chi = 4$.

One reason this general stability might be of interest is if effective launch rate becomes negative, would representing implementation of a program for actively deorbiting more satellites than are launched per year. In this case, $\chi < 0$, and if $\rho > -1$ the equilibrium point becomes unstable. Another reason this general stability might be of interest is if an orbital fragment collection program were implemented to make $\beta < 0$ such that $|\beta|$ is comparable to α (if $|\beta| \ll \alpha$, the $Q \sim 1$ approximation still holds). In this case, the equilibrium point could also become unstable if ρ becomes negative enough to cross the curved black line in Figure 12.

Time to Peak as a function of χ and ρ . The final point in this section is based on a practical consideration. While equilibrium and stability are analytically interesting and helpful, they deal with the final state of the system and shed little light on the time dimension of the problem. In the case of orbital debris proliferation in LEO, it may take hundreds of years to approach equilibrium. In all cases studied so far, however, a catastrophic event – the peak and sudden decrease of intact orbiting satellites – occurs well before long-term equilibration.

Figure 13 illustrates this concept for a family of solutions with varying values of χ but identical initial conditions ($M_0 = 1.138, m_0 = 0.3861$) and values of ρ ($\rho = 0.007$). Note in the upper plot that the time at which the number of satellites in LEO peaks (i.e., M_{max}) decreases as χ increases. This is not captured by equilibrium considerations.

One advantage of the simplified model in this work is that it completely describes the dynamics of the changes in N and n (or M and m) in terms of two parameters rather than the five in the simplified [dimensional] model. That is, specification of χ and ρ (plus initial conditions) determines a unique solution. Using the standard $M_0 = 1.138, m_0 = 0.3861$

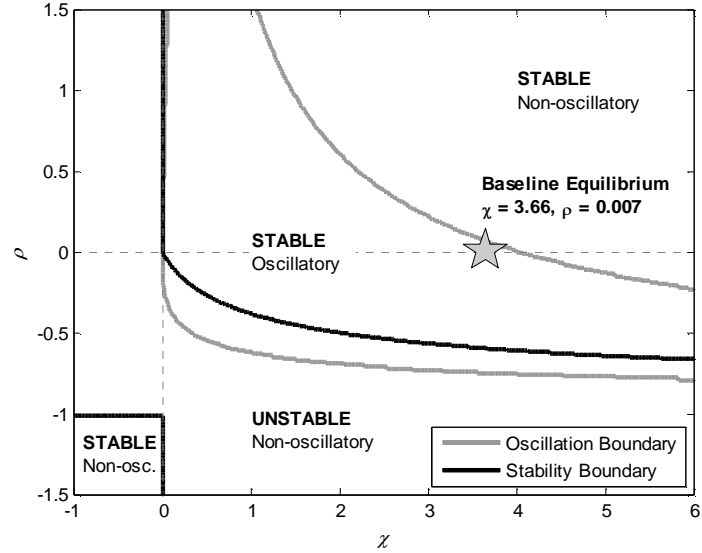


Figure 12. General stability of the equilibrium point as a function of χ and ρ .

initial conditions used throughout this work, these unique solutions have been computed for a range of χ and ρ values, shown in Figure 14. For example, in the upper plot the gray star indicates that the nondimensional time at which the baseline case reaches its maximum satellite population is $s = 0.8$. Using $p = 130$ years, this translates into $t = 104$ years, plotted in the lower plot.

Note also that time to peak decreases as χ increases. For example, if χ increases to $\chi = 7$, the nondimensional time to peak is halved to $s = 0.4$. Such an increase in χ could occur by doubling x , a , or a , or by multiplying p by 1.414. If the increase in χ is due to the doubling of x , a , or a , the dimensional time to peak becomes $t = 52$ years. If the increase is due to a change in p , this changes both χ and the scaling relationship between s and t (since $s = t/p$). In this case, the dimensional time to peak becomes $t = 74$ years. This illustrates the use of Figure 14 for conducting sensitivity analysis and first-order trade studies. Note that, while χ is the dominant parameter governing this time-to-peak metric, the slopes in the contours of Figure 14 illustrate that the parameter ρ is still important.

IMPLICATIONS FOR ORBITAL DEBRIS MITIGATION

With a new model now available and thoroughly examined, the obvious question becomes: What can the model tell us about how to improve the future of orbital debris proliferation? This section addresses this question in three parts. First, strategies for improving the equilibrium state are discussed. Second, strategies for extending the time-to-peak metric are discussed. Third, the results of a simulation are shown in which modest improvements are made as discussed in the first two discussions.

Discussion in this section will be guided by the simplified model presented above. As a result, focus will be on the following five parameters, and particularly on the first two:

- **Effective Launch Rate (a)** is one of the most easily modified by government policies and programs. Reducing this number could occur by reducing the number of satellites placed in orbit per year (e.g., launch a few large instead of multiple smaller satellites) or by actively deorbiting intact satellites.
- **Fragments per Launch (β)** is also susceptible to domestic and international policy and has indeed been decreasing as policies have been introduced to vent excess propellant from upper stages after launch (reducing the likelihood of an upper stage explosion). This parameter also accounts for anti-satellite missile tests, the debris from which is effectively averaged over the launches between tests. It can also account for actively deorbiting fragments (for example, through masses of aerogel deployed by dedicated “sweeper” spacecraft⁴).
- **Intact-Fragment Collision Probability (x)** is difficult to change, although Eqs. (9)-(10) provide some insight into how this might be done. While average speed is largely determined by orbital mechanics and the volume of the LEO belt is fixed, satellites could be made smaller to reduce cross-sectional area. Additionally, if active collision avoidance is employed, this would manifest itself through reductions in x . For example, if 10% of collisions with debris could be both predicted and avoided, x would be effectively reduced by 10%.

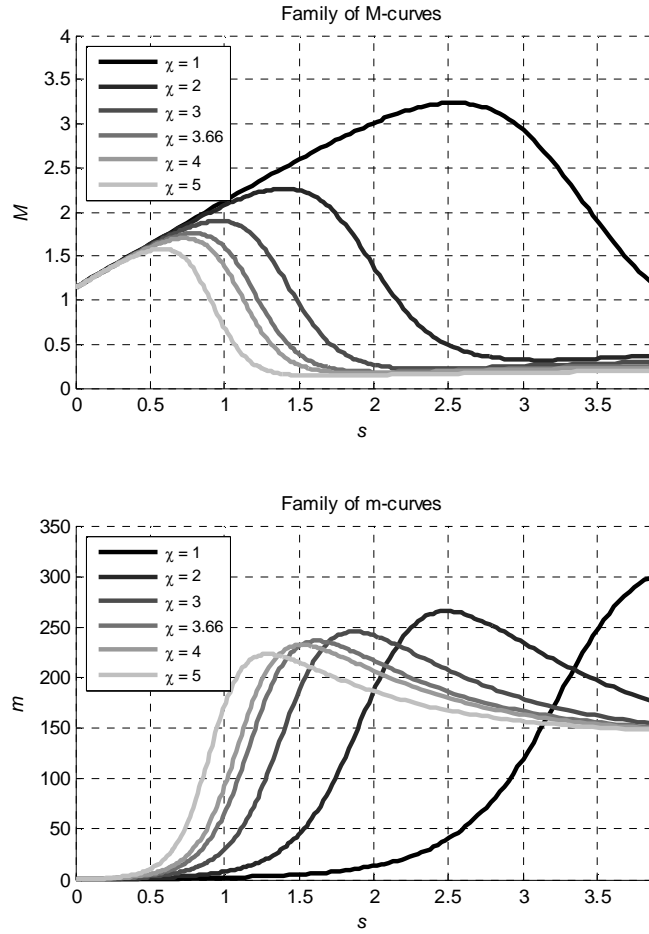


Figure 13. Family of simulations for the same initial conditions but varying χ values ($\rho = 0.007$). In the upper plot, note the backward shift of the time at which M_{max} occurs as χ increases.

Note, however, that any such reduction on x mathematically applies to all intact satellites and not just those that are currently active and controllable.

- **Average Fragment Orbital Lifetime (p)** is also difficult to change, but theoretically could be accomplished if debris fragments are changed to have larger cross-sectional areas or lower mass, are distributed more toward lower altitudes, or are subjected to larger atmospheric densities. For example, some creative proposals have included locally heating the atmosphere to produce high-density bulges out to satellite altitudes.⁴
 - **Fragments per Intact-Fragment Collision (α)** is a third parameter difficult to change. However, this might be modified if satellites are manufactured with structures or shielding designed to fracture into fewer pieces.

Note that these are the only parameters that appear in the simplified model and are the primary means of influencing orbital debris proliferation. As shown earlier, the other eleven parameters in Eqs. (3)-(4) are unimportant for describing equilibrium or time-to-peak behavior.

Sustainability: Improving the Equilibrium State

The first question this model can help answer is how the equilibrium state (the number of satellites and fragments in LEO) can be improved through action by governments, satellite manufacturers, and satellite users. While equilibrium is reached only after a long period of time, it is useful as an indicator of the sustainability of use of LEO.

Throughout the following discussion, it is assumed $\beta \ll \alpha$ so the equilibrium point is negligibly affected by β . That is, it is assumed the number of fragments created per launch (or destroyed per launch, if $\beta < 0$) is much smaller than the number of fragments created per collision between a fragment and a satellite. Recall the baseline value for β/α is 0.007 and that worldwide mitigation efforts have in general *reduced* this number by reducing β . Thus, $\beta \ll \alpha$ is a reasonable assumption, provided anti-satellite tests (which would effectively increase β) remain uncommon.

Increasing Equilibrium Satellite Capacity. One measure of the sustainability of LEO satellite operations is the total long-term (equilibrium) capacity for intact satellites. In terms of the model in this study, this is represented by N^* , an approximate formula for which is shown in Eq. (25). While there is no clear ideal long-term value of N^* , some insight can be gained by solving for the conditions required to make N^* equal to the number of intact satellites in orbit today ($N_0 = 4650$, from Table 1). In other words, what conditions would need to exist to make the current number of intact satellites sustainable?

Figure 15 shows N^* as a function of x and $p\alpha$. Note that, according to Eq. (25), the only parameters that have a significant influence on N^* are x , p , and α ; however, as noted earlier,

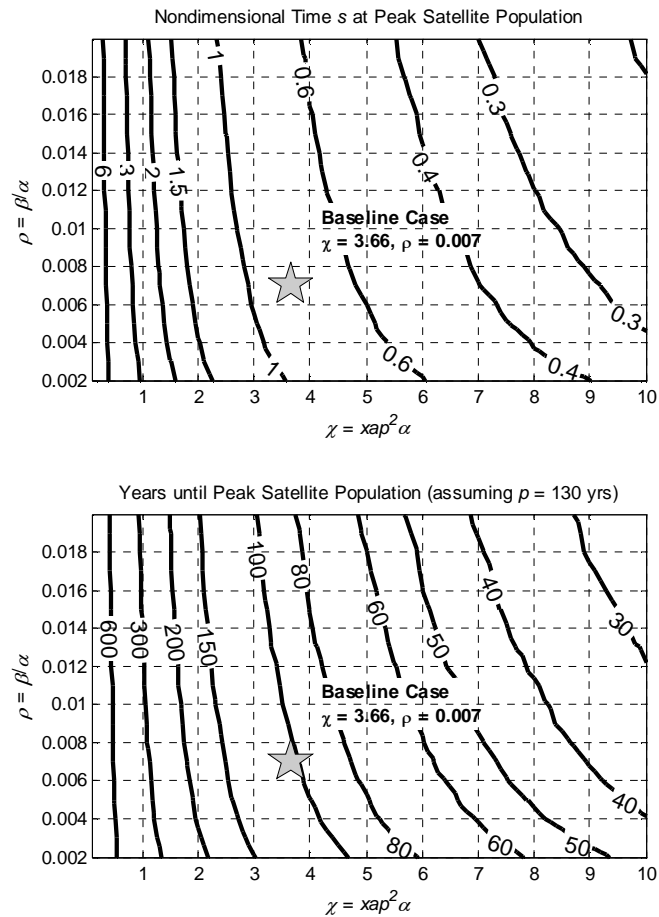


Figure 14. Time at which the LEO intact satellite population peaks, referenced to 2009 and generated using the simplified model of Eqs. (20)-(21). Initial conditions are $M_0 = 1.138$, $m_0 = 0.3861$.

* The case $\beta < 0$ with $|\beta|$ not much smaller than α (e.g., for a massive debris fragment cleanup effort) is discussed later.

these three parameters are difficult to change. As Figure 15 shows, if it were impossible to change these three parameters from their nominal values in Table 1, the equilibrium number of intact satellites in LEO would be about 1100, less than 25% of the number in orbit today.

Perhaps the most easily envisionable way of influencing N^* is through changing x , the annual per-fragment probability of collision for an intact satellite. As mentioned earlier, this may most easily be influenced by changing the cross-sectional area of satellites. Figure 15 shows that if the current number of intact satellites is to be the equilibrium value, x must be reduced to 1.6×10^{-10} to 2.1×10^{-10} per year per fragment, depending on whether $p\alpha$ remains the same or is reduced by 20% (for example, by reducing both p and α by approximately 10%), respectively. This corresponds to a reduction in effective cross-sectional area from 3.77 m^2 to between 0.87 m^2 and 1.15 m^2 . This translates into reducing satellite length scales by roughly a factor of two and thus reducing volume by a factor of 8 while presumably retaining the same functionality. Clearly this could be a daunting task. The alternative of reducing x by a factor of four through active collision avoidance is equally daunting; even if collisions could somehow be avoided for all 560 active satellites in LEO,⁴ there would still be over 4,000 inactive satellites (88% of the population) for which no control is available.

While it may be daunting to meet this goal on x completely, there is still benefit to small reductions. For example, if the typical 2.2 m diameter assumed earlier is reduced by 2 cm (about 1%), N^* increases by about 12 satellites. This suggests development efforts aimed at miniaturization may be helpful from an orbital debris risk perspective. A more formal statement on this is given by the partial derivative $\partial N^*/\partial x$ in Eq. (31).

Minimizing Equilibrium Collision Probability. A second measure of sustainability is the equilibrium probability of collision for intact satellites. This metric is perhaps more important than the intact satellite equilibrium capacity because it defines the minimum level of risk tolerance individuals or organizations must have in order to decide to use satellites over other alternative methods of communication, reconnaissance, or remote sensing, for example.

This equilibrium annual collision probability, P_{coll}^* , is proportional to n^* through Eq. (32), derived from the gas-dynamics-based Eq. (9).

Figure 16 shows P_{coll}^* plotted as a function of a and $p\alpha$.^{*} Cross-sectional area, average orbital velocity, and LEO volume are assumed fixed. The vertical line in the figure shows the nominal setting of a based on Table 1. The intersection of this line with the black $p\alpha$ line indicates that the nominal equilibrium collision probability is 2.8% per year; if $p\alpha$ can be reduced by 20% (the light gray line), this changes slightly to 2.3% per year. For context, this corresponds to a 20-25% probability of collision (and corresponding loss of satellite) within 10 years and a 29-34% probability within 15 years, well within the expected lifetimes of many satellites. This represents a substantial risk well above risks that already exist for failure due to component malfunctions, and it is questionable whether such a risk would support the continued use of satellites for many applications.

The horizontal line in Figure 16 shows the typical failure rate of LEO satellites after 1 year in orbit (0.93% per year, derived from Reference 14)[†] and can be considered currently accepted by the satellite industry. If the industry might accept an orbital debris collision risk on par with the risk of all other failures, this number serves as an estimate for an

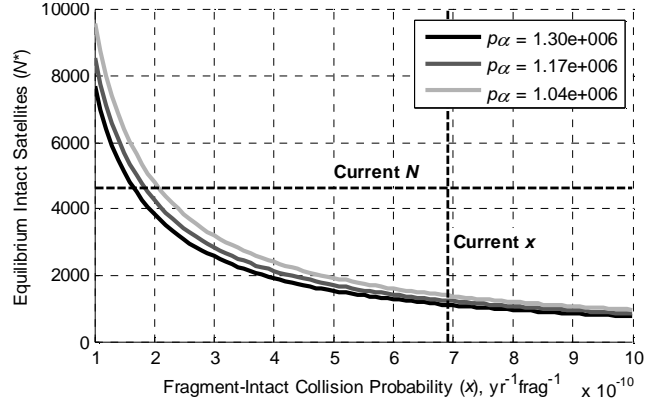


Figure 15. Equilibrium number of intact satellites in LEO as a function of x and $p\alpha$.

$$\frac{\partial N^*}{\partial x} = -\frac{1}{x^2 p(\alpha + \beta)} \sim -\frac{1}{x^2 p\alpha} \quad (31)$$

$$P_{coll}^* = \frac{\sigma_{Nn}\bar{V}}{V} n^* = \frac{\sigma_{Nn}\bar{V}}{V} p\alpha(\beta + \alpha) \sim \frac{\sigma_{Nn}\bar{V}}{V} p\alpha \quad (32)$$

* Note that this collision probability is inherently averaged over all of the LEO volume.

† The model used to generate this estimate is a Weibull distribution model with infant mortality, so this 0.93% per year estimate is on the high side of a currently acceptable failure rate.

appropriate P_{coll}^* target. As Figure 16 shows, this would require reduction of the global LEO launch rate to 10-13 satellites per year. This could involve reducing the number of satellites launched or, for example, continuing to launch 31 per year but actively deorbiting 18-21 satellites per year. Either change is substantial.

Similar to the previous section, it is instructive to take the partial derivative of Eq. (32) with respect to a . This expression, in Eq. (33), indicates $\partial P_{coll}^*/\partial a$ is constant with a . For the nominal values of σ_{Nn} , v , V , p , and α used throughout this study, the this derivative is $\partial P_{coll}^*/\partial a = 0.000898 \text{ yr}^{-1}$. Thus, for every 11-satellite launch rate reduction (or, alternatively, every 11 satellites deorbited per year), the equilibrium annual probability of collision is reduced by nearly 1%.

Buying Time: Delaying Time-to-Peak

As the previous section indicated, creating an acceptable equilibrium state would require substantial changes to the annual satellite launch rate or size of satellites in the LEO population. Ultimately, these changes may be necessary since equilibrium will eventually be reached. However, a reasonable question is whether the time-to-peak (the time before the “crash” in intact satellites) can be delayed while technology development and policy efforts are undertaken to solve the equilibrium problem.

For the following discussion, the baseline model with no sinusoidal forcing and $p = 130$ years is used (Eqs. (14)-(15)). Since negative values of a and β are considered, an additional rule was added to the MATLAB numerical integration to set $dN/dt = 0$ if $N \leq 0$ and $dn/dt = 0$ if $n \leq 0$ to avoid negative numbers of satellites and fragments.

Figure 17 shows how time-to-peak changes as launch rate and debris per launch, the two most easily changeable parameters, are varied over a reasonable range. The baseline case defined by the nominal parameters in Table 1 is marked by the gray star. This indicates that the current peak in the number of intact satellites in LEO occurs in about 97 years, or in the year 2106.* If β is held constant and a is decreased, time-to-peak increases until $a = 19$ satellites/year, at which point time-to-peak is 100 years. As a is further decreased and launch rate becomes very low, time-to-peak decreases until $a = 0$, at which point the maximum population of intact satellites is maximum at $t = 0$ since no satellites are being launched (and some are being destroyed by debris). Thus, decreasing a locally has little effect on delaying time-to-peak. In partial derivative terms, for every launch avoided (or satellite deorbited) per year, 3 months are added to the time-to-peak.

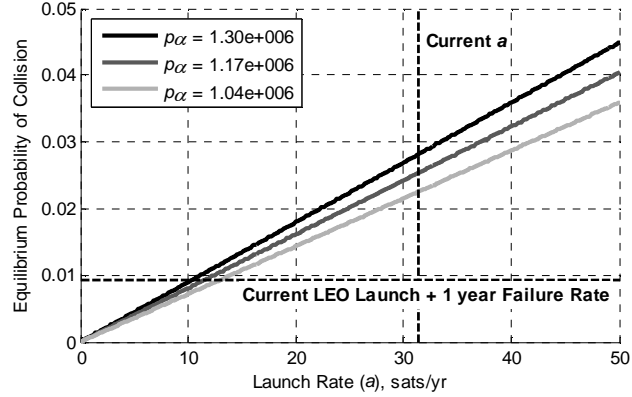


Figure 16. Equilibrium annual probability of collision for intact satellites as a function of a and $p\alpha$.

$$\frac{\partial P_{coll}^*}{\partial a} = \frac{\sigma_{Nn} \bar{v}}{V} p(\beta + \alpha) \sim \frac{\sigma_{Nn} \bar{v}}{V} p\alpha \quad (33)$$

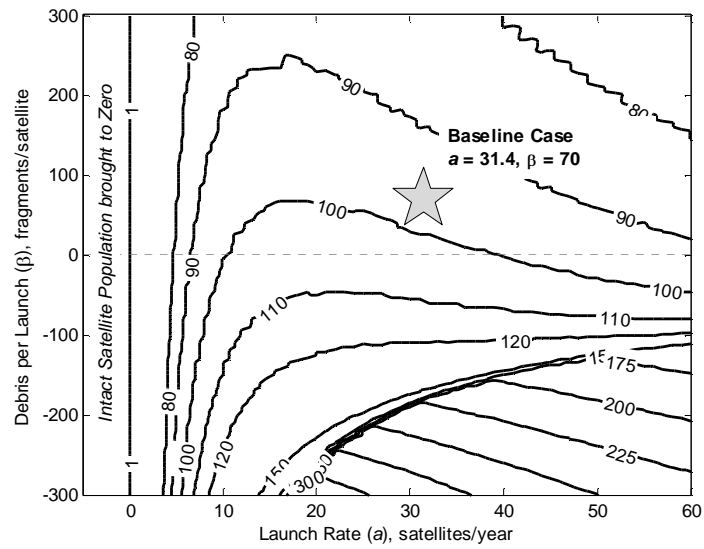


Figure 17. Time to Peak (in years) as a function of launch rate a and debris per launch β .

* Since the no-sinusoid model of Eqs. (14)-(15) is used to generate the results of Figure 17, the nominal time-to-peak is slightly discrepant from the full model of Eqs. (3)-(4). This is the reason for the 2106 vs. 2108 year disagreement.

Turning to the situation where a is held constant and β is decreased appears much more fruitful. Decreasing β to zero (i.e., eliminating debris release per launch, or destroying as much debris as is generated per launch) brings time-to-peak to 103 years. In partial derivative terms, for every debris fragment not released per launch, one month is added to time-to-peak. Decreasing β beyond this, time-to-peak is delayed to 120 years once $\beta = -110$. Such a value for β would require the deployment of systems that are able to “sweep up” 110 debris fragments for every launch of the year. A critical point is reached once $\beta = -190$. Here, time-to-peak rises to over 200 years. Physically, this occurs because at about $\beta = -190$, the fragment population is entirely “cleaned up” at a rate of $\beta a = 5,970$ fragments per year for 60 years. Then, for several decades the fragment population remains zero until the intact satellite population rises enough for the intact-intact collision rate to exceed the maximum “clean up” rate; at this point, the fragment population grows, precipitates additional collisions, and eventually peaks.

One surprising outcome of this time-to-peak analysis is that, unlike the equilibrium discussion in which β had negligible influence and a presented the primary means of reducing long-term risks, the opposite is true. In terms of time-to-peak, a has a minor influence while β presents a potential solution. Further, values of β required for centuries of time-to-peak extension remain within the $|\beta| \ll a$ regime assumed for the simple equilibrium equations earlier.

Example Modest Improvements

The previous sections have highlighted three means of improving the equilibrium and time-to-peak characteristics of the debris proliferation problem: reduction in satellite size (to reduce x), reduction in global launch rate (a), and reduction in fragments released per launch (β). While these primary mechanisms can be tweaked in many ways, presented here is a scenario illustrating the implementation of reasonably ambitious policies for orbital debris mitigation using the model of Eqs. (3)-(4). Here, x is set to $5.585 \times 10^{-10} \text{ yr}^{-1} \cdot \text{frag}^{-1}$ and y is set to $1.109 \times 10^{-9} \text{ yr}^{-1} \cdot \text{sat}^{-1}$, representing a 10% reduction in satellite characteristic length dimensions. The a and b launch rate parameters are set to $\frac{1}{3}$ of their original values, representing policies encouraging $\frac{1}{3}$ of satellite owners to deorbit their satellites at the end of their useful lives. Thus, $a = 20.94$ satellites/year and $b = 5.196$ satellites/year. Finally, β is reduced by half (to $\beta = 35$), representing policies encouraging further limits on launch-related debris. Recognizing that such changes take time to implement, the simulation only begins using the new constants after the year 2019 (at $t = 10$ years), in close agreement with the assumption of Reference 27.

Figure 18 shows the result of implementing these coefficient changes in the nominal model of Eqs. (3)-(4). In the top plot, note that the peak number of intact satellites occurs in the year 2134, 26 years after the original model, and the “crash” following the peak takes about 40 years longer. Additionally, the equilibrium value of the improved-policy model is slightly higher. In the bottom plot, the ramp to the peak amount of debris is slower in the improved-policy version, the peak itself is about 20% lower, and the equilibrium value is about 25% lower, all reflecting lower probabilities of collision for intact satellites. Overall, this illustrates how modest changes to the parameters of the model, for example through debris mitigation policies, can substantially delay or reduce the proliferation of orbital debris.

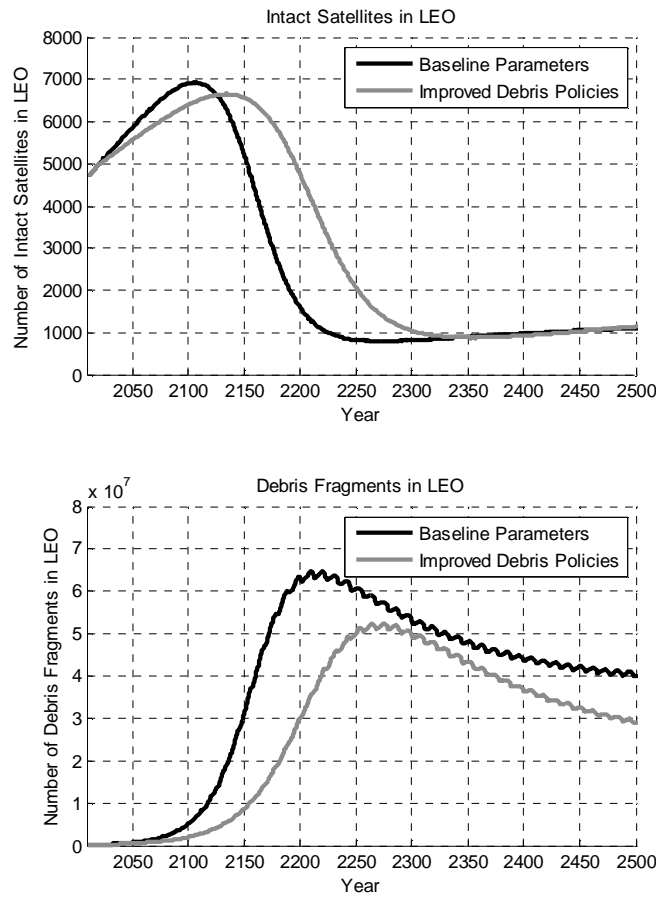


Figure 18. Number of intact satellites and debris fragments in LEO as a function of time, comparing the baseline model to one with modest policy improvements.

CONCLUSION

In summary, this work has extended the model of orbital debris proliferation proposed by Reference 5 while retaining the original model's simple two-equation form. The new model includes effects such as atmospheric drag and collisions between intact satellites, and coefficients have been re-estimated based on current data. Analysis of this new model reveals that although Reference 5 accounted for most major effects, a critical term was missing, namely the reduction in orbiting fragments due to atmospheric drag. This significantly changes the character of orbital debris proliferation from one of unbounded growth to one of eventual equilibrium. Moreover, analysis has shown that this equilibrium point, which did not exist previously, is stable for most practical values of model parameters. Thus, the debris problem becomes less one of bounding the growth of debris and more one of ensuring an acceptable equilibrium.

Without any changes, the current equilibrium state allows only 25% of the intact satellites in orbit today and presents a 2.8% per year risk of catastrophic collision for individual satellites. Methods for improving this equilibrium state have been explored. Two promising options appear to be reducing launch rate (or increasing deorbit rate) and reducing satellite size. While the reductions required to bring the equilibrium satellite capacity and equilibrium collision probability to acceptable levels appear too drastic to be immediately practical, the analysis did suggest small changes in these parameters could provide significant gains. For every centimeter decrease in the average satellite length scale, about 6 satellites are added to the LEO equilibrium satellite capacity. For every 11 satellites actively deorbited (or not launched) per year, equilibrium collision probability for individual satellites is reduced by 1% per year.

With this said, although equilibrium considerations are important because they describe the eventual fate of the LEO satellite population, another important consideration is whether the characteristic "crash" in the satellite population can be delayed while technology development or other policies are implemented. Examination of this time-to-peak metric shows that changes from the current launch rate have a minimal effect on the baseline 97-year time-to-peak, while reductions in the average amount of debris placed into orbit per launch can have a substantial effect. In particular, if 190 pieces of debris or more are collected per launch, time-to-peak could be extended by centuries. This makes a potentially compelling case for the development of spacecraft to catch (or actively deorbit) pieces of debris at the rate of 5,900 pieces per year (i.e., 190 fragments for each of 31 launches per year). While not an easy task, "catch rates" in the hundreds or low thousands of fragments per year do not seem impossible. However, regardless of whether such spacecraft become a reality, reductions in orbital fragments released per launch appear more cost-effective in the short term. For every satellite actively deorbited (or for every launch avoided) per year, time-to-peak is extended by 3 months. According to the data shown here, this same 3-month extension can also be obtained by releasing just three fewer fragments per launch. While further investigation is required, technology development in this area may be justified.

One danger of the results presented here is that they predict the "crash" in the satellite population will happen in roughly 100 years, which might seem to imply the problem should be a low priority. However, all simulations in this work have exhibited this "crash", followed by a high level of risk and low satellite capacity in the aftermath. Orbital debris is a strategic threat to the global space infrastructure, and the space industry's management of the situation will be largely a function of the preparations made and policies implemented decades prior to the event itself.

It is important to note that this study has limitations. For example, this study did not explicitly distinguish between orbital bands, some of which have higher satellite and fragment densities than others. The focus here was on the overall properties of LEO orbital debris proliferation, in order to identify trends, key dependencies, and approximate estimates. For instance, orbital bands with high satellite and fragment densities will likely experience higher annual collision probabilities than the average values used here for all of LEO. Also, this work has assumed continuous variables and equations when in reality satellite launches and collisions are discrete events. Additionally, the use of "space-sweeping" satellites might also be modeled more accurately in the future; for example, it is likely that the "catch rate" would decrease as more fragments are caught, since the fragments would become increasingly more difficult to find. Finally, a useful next step in this model's development would be a rigorous validation against higher-fidelity simulations.

Overall, this work has employed a variety of analytical tools on the practical – and globally critical – problem of long-term debris proliferation in low Earth orbit. It is hoped some of the ideas, methods, and results in this work will find use in the broader community and provide guidance to help inform future decisions on debris mitigation policies and technology investments.

ACKNOWLEDGEMENTS

The author would like to sincerely thank Dr. Maria Westdickenberg in the Georgia Tech School of Mathematics for her input and support throughout this project. In addition, thanks are due to Mr. Thomas Hiriart and Dr. Ryan Rus-

sell in the Georgia Tech School of Aerospace Engineering. Finally, the author would like to acknowledge the support of the Department of Defense through the National Defense Science and Engineering Graduate (NDSEG) Fellowship.

REFERENCES

- ¹ NASA Goddard Space Flight Center, *National Space Science Data Center Spacecraft Query* [database], Available at: <http://nssdc.gsfc.nasa.gov/nmc/SpacecraftQuery.jsp> [29 Sept. 2009].
- ² “Orbital Debris Education Package,” NASA JSC Orbital Debris Program Office, Available at: <http://www.orbitaldebris.jsc.nasa.gov/library/EducationPackage.pdf> [29 Sept. 2009].
- ³ E. Stansbery, ed., ‘‘NASA Orbital Debris FAQs,’’ NASA JSC Orbital Debris Program Office, 7 July 2009, Available at: <http://www.orbitaldebris.jsc.nasa.gov/faqs.html> [29 Sept. 2009].
- ⁴ M.H. Kaplan, “Survey of Space Debris Red. Methods,” AIAA 2009-6619, Space 2009, Pasadena, 14-17 Sept. 2009.
- ⁵ P. Farinella and A. Cordelli, ‘‘The Proliferation of Orbiting Fragments: A Simple Mathematical Model,’’ *Science & Global Security*, Vol. 2, 1991, pp. 365-378.
- ⁶ Center for Space Standards & Innovation, *SOCRATES: Satellite Orbital Conjunction Reports Assessing Threatening Encounters in Space* [online database], Available at: <http://celestrak.com/SOCRATES/> [4 Oct. 2010].
- ⁷ D.J. Kessler and B.G. Cour-Palais, ‘‘Collision Frequency of Artificial Satellites: The Creation of a Debris Belt,’’ *Journal of Geophysical Research*, Vol. 83, 1978, pp. 2637-2646.
- ⁸ D.L. Talent, ‘‘Analytic Model for Orb. Debris Env. Mgmt.’’, *J. Spacecraft & Rockets*, Vol. 29, 1992, pp. 508-513.
- ⁹ A. Cordelli, P. Farinella, L. Anselmo, C. Pardini, and A. Rossi, ‘‘Future Collisional Evolution of Earth-orbiting Debris,’’ *Advances in Space Research*, Vol. 13, 1993, pp. 215-219.
- ¹⁰ A. Rossi, A. Cordelli, P. Farinella, and L. Anselmo, ‘‘Collisional evolution of the Earth’s orbital debris cloud,’’ *Journal of Geophysical Research*, Vol. 99, 1994, pp. 195-210.
- ¹¹ H.G. Lewis, G.G. Swinerd, et. al., ‘‘The fast debris evolution model,’’ *Adv. in Space Res.*, Vol. 44, 2009, pp. 568-578.
- ¹² T.H. Hiriart and J.H. Saleh, ‘‘Cyclical in the Space Industry: Myth or Reality? Times Series Analysis, Periodogram, and Identification of Trends and Cyclical Patterns,’’ AIAA 2009-6478, Space 2009, Pasadena, 14-17 Sept. 2009.
- ¹³ D.H. Hathaway, ‘‘The Sunspot Cycle,’’ NASA Marshall Space Flight Center Solar Physics Group, 5 Oct. 2009, Available at: <http://solarscience.msfc.nasa.gov/SunspotCycle.shtml> [1 Nov. 2009].
- ¹⁴ T. Hiriart, J. Castet, J. Lafleur, and J. Saleh, ‘‘Comparative Reliability of GEO, LEO, and MEO Satellites,’’ IAC-09.D1.6.1, 60th International Astronautical Congress, Daejeon, 12-16 Oct. 2009.
- ¹⁵ W.J. Larson and J.R. Wertz (eds.), *Space Mission Analysis and Design*, 3rd ed., Microcosm, El Segundo, 1999.
- ¹⁶ J.M. Lafleur and J.H. Saleh, ‘‘GT-FAST: A Point Design Tool for Rapid Fractionated Spacecraft Sizing and Synthesis,’’ AIAA 2009-6563, AIAA 2009 Conference and Exposition, Pasadena, 14-17 Sept. 2009.
- ¹⁷ G.D. Badwhar and P.D. Anz-Meador, ‘‘Determination of the Area and Mass Distribution of Orbital Debris Fragments,’’ *Earth, Moon, and Planets*, Vol. 45, 1989, pp. 29-51.
- ¹⁸ W.G. Vincenti and C.H. Kruger, Jr., *Introduction to Physical Gas Dynamics*, Krieger, Malabar, 1965, Chap. 1.
- ¹⁹ NASA JPL, *Mission and Spacecraft Library* [database], 1999, Available at: <http://msl.jpl.nasa.gov/> [8 Oct. 2010].
- ²⁰ NASA MSFC, ‘‘Chandra X-Ray Observatory Quick Facts,’’ Fact Sheet FS-1999-09-111-MSFC, Aug. 1999, Available at: http://www.nasa.gov/centers_marshall/news/background/facts/cxoquick.html [8 Oct. 2010].
- ²¹ M. Suzuki, ‘‘Description of Mission,’’ TOPEX/Poseidon, 11 Feb. 1999, Available at: <http://www.tsgc.utexas.edu/spacecraft/topex/stats.html> [8 Oct. 2010].
- ²² C.L. Parkinson, A. Ward, and M.D. King, *Earth Science Reference Handbook*, NASA GSFC, 2006, pp. 157-161.
- ²³ Northrop Grumman Space & Mission Systems, ‘‘Northrop Grumman Spacecraft Guide,’’ Rept. 99K93B, Mar. 2005.
- ²⁴ J. Perbos, ‘‘Jason-1: Satellite and System Perf., One Year After Launch,’’ *Aviso Newsletter*, Vol. 9, 2003, pp. 4-5.
- ²⁵ N.L. Johnson, E. Stansbery, D.O. Whitlock, K.J. Abercromby, and D. Shoots, ‘‘History of On-Orbit Satellite Fragmentations,’’ NASA/TM-2008-214779, Houston, June 2008.
- ²⁶ Shoots, D., NASA Johnson Space Center Orbital Debris Program Office, E-mail Communication, 26 Oct. 2009.
- ²⁷ J.C. Liou, N.L. Johnson, and N.M. Hill, ‘‘Controlling the growth of future LEO debris populations with active debris removal,’’ *Acta Astronautica*, Vol. 66, 2010, pp. 648-653.